Available online at www.sciencedirect.com
SCIENCE DIRECT
Journal of Membrane Science 280 (2006) 849–855
journal of MEMBRANE SCIENCE
www.elsevier.com/locate/memsci

Oxygen permeation through a $Ce_{0.8}Sm_{0.2}O_{2-\delta}$–$La_{0.8}Sr_{0.2}CrO_{3-\delta}$ dual-phase composite membrane

Jianxin Yi [a], Yanbo Zuo [a], Wei Liu [a], Louis Winnubst [a,b], Chusheng Chen [a,*]

[a] *Laboratory of Advanced Functional Materials and Devices, Department of Materials Science and Engineering, University of Science and Technology of China, Hefei, Anhui 230026, PR China*
[b] *Inorganic Materials Science, Faculty of Science and Technology and MESA+ Research Institute for Nanotechnology, University of Twente, P.O. Box 217, 7500 AE Enschede, The Netherlands*

Received 4 November 2005; received in revised form 1 March 2006; accepted 3 March 2006
Available online 12 March 2006

Abstract

A composite of oxygen ion conducting oxide $Ce_{0.8}Sm_{0.2}O_{2-\delta}$ (60 vol.%) and electron conducting oxide $La_{0.8}Sr_{0.2}CrO_{3-\delta}$ was prepared by sintering a powder compact at a temperature of 1550 °C. No significant reaction between the two constituent oxides was observed under preparation and oxygen permeation conditions. Appreciable oxygen permeation fluxes through the composite membrane were measured at elevated temperatures with one side of it exposed to the ambient air and the other side to a flowing helium gas stream. The oxygen flux initially increased with time, and took a long time to reach a steady value. A steady oxygen permeation flux as high as 1.4×10^{-7} mol cm^{-2} s^{-1} was obtained with a 0.3 mm thick membrane at 950 °C under a relatively small oxygen partial pressure difference of 0.21 bar/0.0092 bar. It was revealed that the overall oxygen permeation process was mainly limited by the transport in the bulk of the membrane in the range of the membrane thickness greater than ∼1.0 mm, and the limitation by the surface oxygen exchange came into play at reduced thickness of ∼0.6 mm.

Keywords: Composite membrane; Oxygen permeation; Mixed conductor; Lanthanum chromite; Ceria

1. Introduction

Mixed oxygen ion and electron conductors have received considerable attention for their potential applications in oxygen separation and other oxygen-based industrial processes as partial oxidation of methane (POM) into synthesis gas [1–17]. Currently, most investigated mixed conductors are single-phase perovskite oxide (Ln, A)(Co, Fe, B)$O_{3-\delta}$ (Ln = rare earth elements; A = Ca, Sr, Ba; B = transition metal elements or Ga). These materials possess high oxygen permeability [5–8], but the long-term stability and mechanical strength under a large oxygen gradient are problematic for most of the oxides [3–5]. An exception is Fe-doped $LaGaO_3$, which has been reported to exhibit excellent stability, but the use of expensive Ga may limit its application [6]. Another type of mixed conductors is a dual-phase composite, which allows oxygen ions and electrons to transport through different phases. In most of the dual-phase composites reported, noble metals such as Ag, Au or Pd are used as the electron-conducting phase [9–11]. Recently, good electron conducting oxides such as $La_{0.8}Sr_{0.2}Fe_{0.8}Co_{0.2}O_{3-\delta}$, $La_{0.7}Sr_{0.3}MnO_{3-\delta}$, $Gd_{0.7}Ca_{0.3}CoO_{3-\delta}$ have also been used to make composites with the oxygen ion conducting oxides such as $Ce_{0.8}Gd_{0.2}O_{2-\delta}$ and doped $LaGaO_3$ [12–17]. These composites show considerable oxygen permeability as expected, but for most of them the long term stability of the contained electron conducting oxides in strongly reducing atmosphere and the chemical compatibility with the ion conducting oxides are expected to present problems [3,5,13–15].

It is known that Sm-doped ceria, which is widely used as solid electrolyte in intermediate temperature solid oxide fuel cells (SOFCs), exhibits high oxygen ionic conductivity and good chemical stability [18]. It is also known that Sr-doped $LaCrO_3$ has been used as interconnector in SOFCs for its excellent stability in both oxidizing and reducing atmospheres and high electric conductivity at elevated temperatures [19]. These two oxides have been reported to exhibit similar sintering temperature and thermal expansion coefficient as well as good chemical compatibility [20–22]. Thus a composite made of these two oxides may

* Corresponding author. Tel.: +86 551 3602940; fax: +86 551 3601592.
E-mail address: ccsm@ustc.edu.cn (C. Chen).

0376-7388/$ – see front matter © 2006 Elsevier B.V. All rights reserved.
doi:10.1016/j.memsci.2006.03.011

have acceptable chemical stability and mechanical strength. In the present paper, the preparation, microstructural characterization and oxygen permeability under air/helium gradient of a composite membrane consisting of $Ce_{0.8}Sm_{0.2}O_{2-\delta}$ (60 vol.%) and $La_{0.8}Sr_{0.2}CrO_{3-\delta}$ are reported.

2. Experimental

2.1. Sample preparation and characterization

Fluorite $Ce_{0.8}Sm_{0.2}O_{2-\delta}$ (SDC) powders were prepared by an oxalate complexation–precipitation route. $Ce(NO_3)_2{\cdot}6H_2O$ (>99%) and Sm_2O_3 (>99.99%) powders were respectively dissolved in deionized water and a dilute nitric acid solution and subsequently mixed in the desired cation stoichiometry. The mixed solution was slowly dripped into an oxalic acid solution under intensive stirring, yielding an oxalate precipitate. The oxalate was converted to SDC powder by calcination at 800 °C for 2 h. Perovskite $La_{0.8}Sr_{0.2}CrO_{3-\delta}$ (LSC) powders were synthesized via a conventional solid state reaction route. Appropriate amounts of $SrCO_3$ (>99%), La_2O_3 (>99.99%), Cr_2O_3 (>99%) were weighed and ball-milled. The mixture was calcined at 900, 1100 and 1300 °C for 10 h with intermittent ball-milling. The as-obtained SDC and LSC powders were mixed in a mortar at a weight ratio of 63:37 (volume ratio 60:40) and carefully ground. The powder mixture was uni-axially pressed at 150 MPa, subsequently cold isostatically pressed at 300 MPa, and sintered in ambient air at 1550 °C for 10 h to obtain pellets with a diameter of ∼12.5 mm. Densities of the sintered samples were determined to be 88–90% of the theoretical density using Archimedes method in mercury. The theoretical density of the composite was calculated from the lattice constants of the two oxide phases derived from XRD patterns. The membranes were polished before subjected to the tests to avoid the possible effect of surface contamination formed during preparation. Phase composition of the composite was characterized by XRD (Philips X'Pert Pro Super, Cu Kα). Microstructure examination and elemental analysis were performed by SEM (JEOL JSM-6700F) coupled with INCA energy-dispersive X-ray spectroscopy (EDX). The electric conductivity of the composite was measured using AC impedance spectroscopy (CHI604A). For the measurement, a sample of thickness 1.5 mm was painted with Pt paste on both sides and then fired at 850 °C for 10 min. The frequency ranged from 100 kHz to 1 Hz.

2.2. Oxygen permeation

Experimental details on oxygen permeation measurements are referred to Ref. [10]. Disk-shaped samples were machined to required thicknesses and ultrasonically cleaned in ethanol, then sealed to the end of an alumina tube at 1000 °C using a glass ring to form a permeation cell. After sealing, the temperature was lowered to 900 °C, and air was fed at one side of the sample, while helium was led over the other side to sweep away the permeated oxygen. During the permeation measurement, the oxygen partial pressure was kept constant at 0.21 bar at the feed side ($P_{O_2}(h)$), while the oxygen partial pressure of the effluent at the permeate side ($P_{O_2}(l)$) varied between 10^{-2} and 10^{-4} bar depending on the amount of permeated oxygen and the sweeping rate of the helium. The composition of the effluent stream at the permeate side was analyzed by an online gas chromatograph (GC9750). The oxygen fluxes were corrected for any oxygen leakage through the glass sealant or imperfection in the pellet by measuring the concentration of nitrogen in the effluent stream. The amount of oxygen leakage is typically less than 5% of the total amount of the permeate oxygen. The temperature range was 850–1000 °C. For comparison, the oxygen permeation through membranes coated with porous Pt layer on both feed and permeate sides was also measured; preparation of these surface-modified membranes is similar to that of the sample for the impedance measurement.

3. Results

3.1. Phase composition and microstructure of the as-sintered composite membranes

XRD analysis on the sintered and polished sample shows that the composite consists of SDC and LSC oxides (Fig. 1). Fig. 2a shows the backscattered electron SEM image of the polished composite. Apparently, the sample is composed of two types of grains with different grey levels, along with some pores corresponding to the black areas in the SEM image (Fig. 2a). EDX spot analysis reveals that the light grains contain mainly Ce and Sm elements (Fig. 2b), while the dark grains contain mainly La, Sr and Cr (Fig. 2c). In combination with the XRD analysis, the light and dark grains in the composite are identified as SDC and LSC phase, respectively. These two phases have grain sizes of 1–4 and ∼1 μm, respectively, and are homogeneously distributed in the composite.

3.2. Oxygen permeation

Oxygen permeation through the composite was measured at elevated temperatures upon applying a differential oxygen

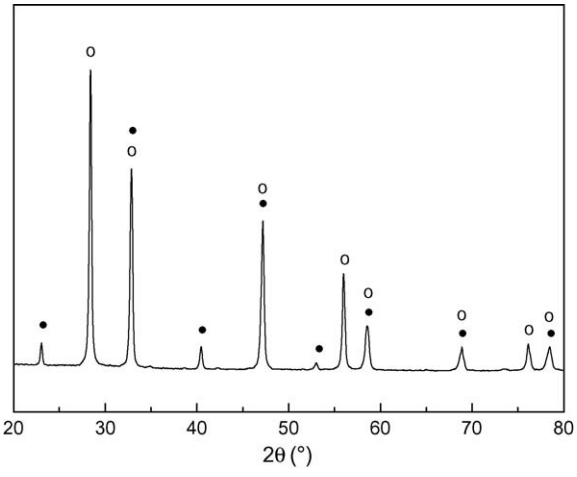

Fig. 1. XRD pattern of polished composite membrane: (○) $Ce_{0.8}Sm_{0.2}O_{2-\delta}$; (●) $La_{0.8}Sr_{0.2}CrO_{3-\delta}$.

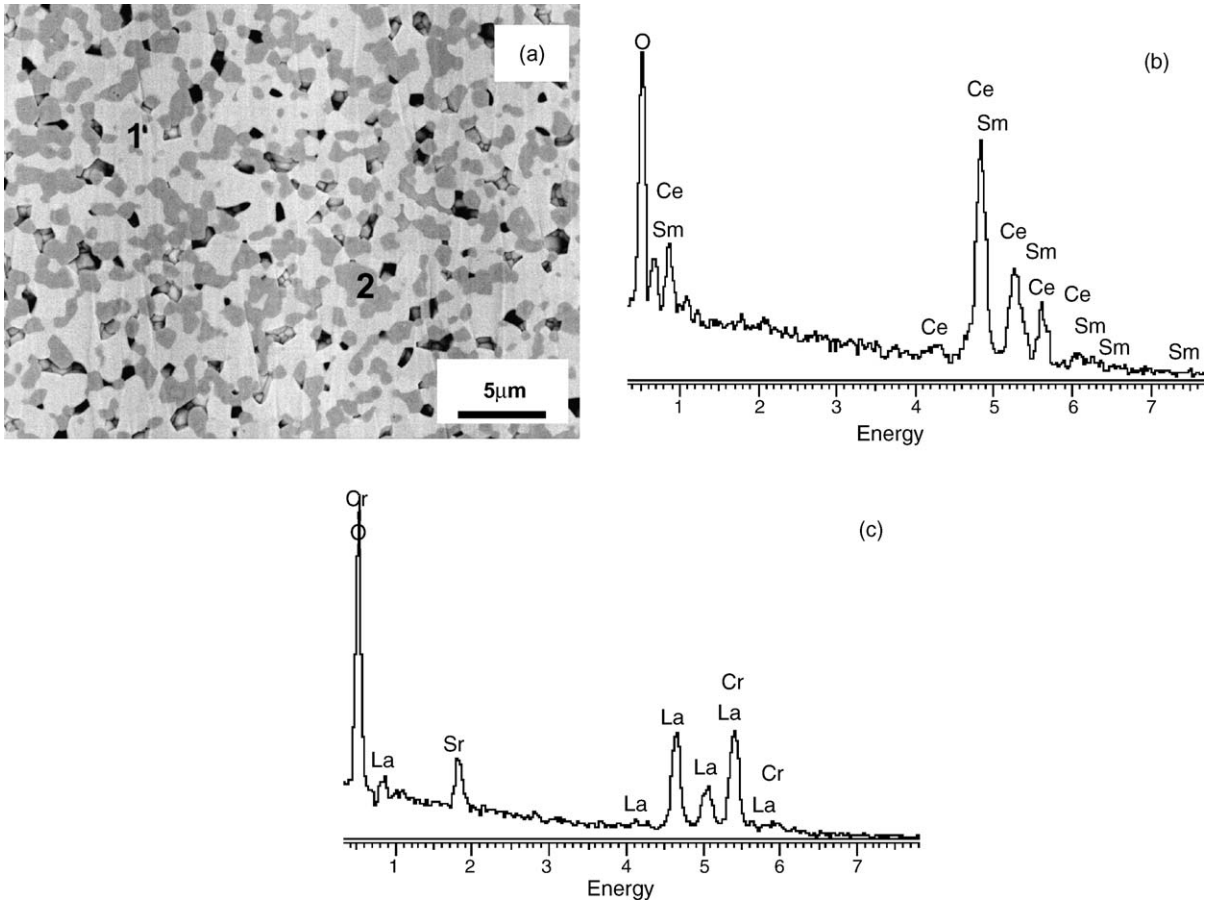

Fig. 2. (a) Backscattered electron image (top view) of a polished membrane, (b) and (c) EDX spot analysis on the light and dark grains, respectively. (1) $Ce_{0.8}Sm_{0.2}O_{2-\delta}$, (2) $La_{0.8}Sr_{0.2}CrO_{3-\delta}$ phase, black holes in (a) correspond to pores in the sample.

partial pressure by exposing one side of the membrane to air and the other side to flowing helium. It was found that the oxygen permeation took a long time to reach a steady state. For a membrane of thickness 1.0 mm at 900 °C, it took about 50 h for the flux to increase from 2.9×10^{-8} to 5.7×10^{-8} mol cm^{-2} s^{-1} (Fig. 3). To find the cause for this time-dependent behavior, the permeation measurement was interrupted for 85 h by removing the oxygen partial pressure difference across the membrane, i.e., replacing the flowing helium at the permeate side with flowing air (while keeping the temperature at 900 °C). It turned out that when the oxygen partial pressure difference was re-applied to the membrane by switching back to the flowing helium, similar time-dependent oxygen permeation behavior appeared: the flux changed from 3.0×10^{-8} to 5.7×10^{-8} mol cm^{-2} s^{-1} within 50 h of operation, and it further rose to 6.2×10^{-8} mol cm^{-2} s^{-1} in a time period of 45 h. It was also found that the time required for the flux to attain a steady value was shortened to several hours with a membrane covered with a porous Pt layer on both feed and permeate sides, although the flux is somewhat lower than that for the uncoated sample, which is possibly due to the sintering or other changes of the covered Pt layer at high temperatures.

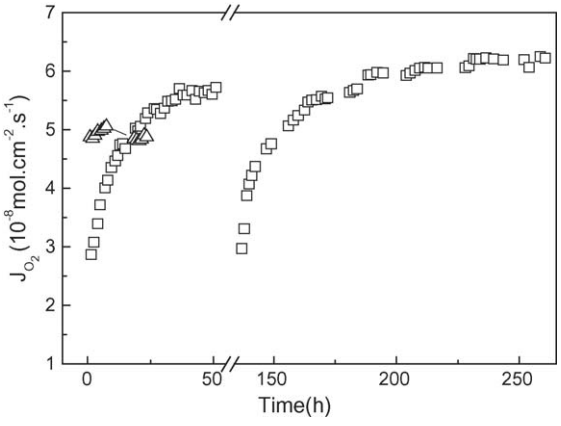

Fig. 3. Time dependence of oxygen flux at 900 °C for (□) uncoated and (△) Pt-coated membrane of thickness 1.0 mm. For the uncoated sample, oxygen permeation measurement was interrupted for 85 h by exposing both sides of the membrane to flowing air (represented by the break in the figure).

Fig. 4 shows the steady oxygen permeation flux (J_{O_2}) of the composite membranes with various thicknesses. It can be seen that the flux increases with temperature as expected. The apparent activation energies for oxygen permeation were calculated to be 129.5 ± 8.3 and 122.6 ± 6.0 kJ mol^{-1} for membranes with thickness of 1.7 and 0.3 mm, respectively. The oxygen flux increases significantly with decreasing membrane thickness. For a membrane of thickness 1.7 mm measured at 950 °C the flux was 4.6×10^{-8} mol cm^{-2} s^{-1} at $P_{O_2}(l)$ of 0.0028 bar, but for a thinner membrane of thickness 0.3 mm, a much larger

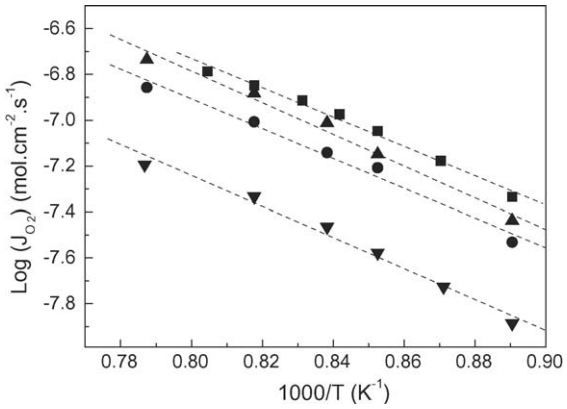

Fig. 4. Temperature dependence of oxygen permeation flux through membranes with thicknesses of (▼) 1.7 mm, (●) 1.0 mm, (▲) 0.6 mm, (■) 0.3 mm. Dashed lines are guides to the eye.

flux of 1.4×10^{-7} mo cm^{-2} s^{-1} at $P_{O_2}(l)$ of 0.0092 bar. These flux values are twice as large as that for $SrFeCo_{0.5}O_{3.25-\delta}$ with comparable thickness measured under similar experimental conditions [23].

Oxygen permeation through the membranes involves exchange of oxygen across the gas/solid interface, transport of oxygen ions through the SDC phase and counter transport of electrons in the LSC phase. In accordance with this transport scheme, the oxygen permeation cell can be essentially regarded as an internally short-circuited electrochemical cell. The driving force for oxygen permeation can be expressed as $E = \frac{RT}{4F} \ln \frac{P_{O_2}(h)}{P_{O_2}(l)}$, where F is the Faraday constant, and the oxygen permeation flux normalized by the driving force is called permeance $F_{O_2} = \frac{J_{O_2}}{E}$ [9]. Fig. 5 shows the permeance against the reciprocal of the membrane thickness (L) at 950–850 °C. Obviously, in the range of the membrane thickness greater than 1.0 mm, F_{O_2} increases proportionally with $1/L$, revealing that the overall oxygen permeation process is mainly limited by the transport of oxygen ions in the bulk of the membrane. But in the range of thickness less than ~0.6 mm, the decrease of the membrane thickness does not lead to significant increase in F_{O_2},

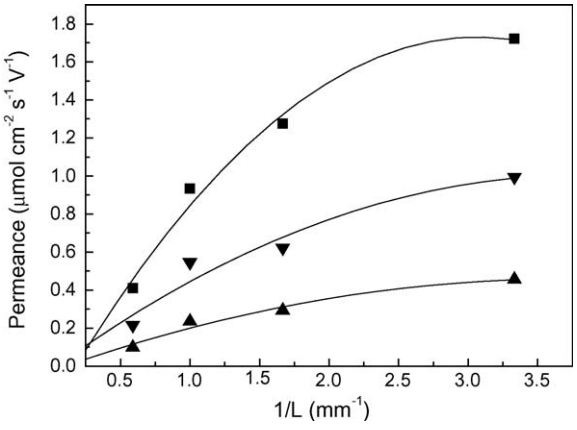

Fig. 5. Thickness dependence of oxygen permeance at temperature of (■) 950 °C, (▼) 900 °C, (▲) 850 °C. Solid lines are guides to the eye.

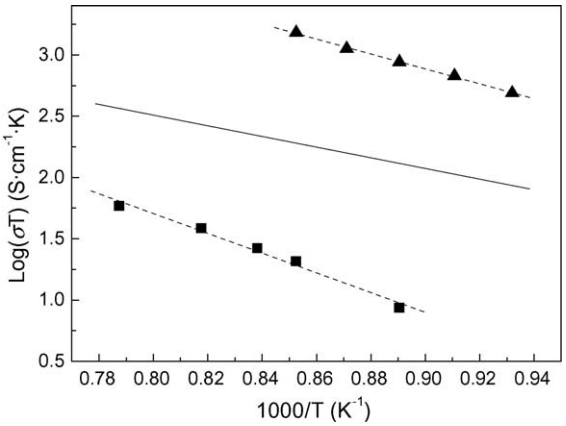

Fig. 6. Arrhenius plots of (■) ambipolar and (▲) total electric conductivity for the composite, (—) oxygen ionic conductivity for single-phase $Ce_{0.8}Sm_{0.2}O_{2-\delta}$ from Ref. [24] (derived from impedance measurements). Dashed lines are guides to the eye.

indicating that the surface exchange kinetics has started to limit the overall oxygen permeation process.

It has been established that when the oxygen permeation is in the bulk-controlled region the permeance is related to the ambipolar conductivity σ_{amb} according to $F_{O_2} = \frac{\sigma_{amb}}{4FL}$, where $\sigma_{amb} = \frac{\sigma_i \sigma_e}{\sigma_i + \sigma_e}$, σ_e and σ_i are the electronic and oxygen ionic conductivity, respectively [9]. Fig. 6 gives the Arrhenius plot of σ_{amb} derived from the permeance for SDC–LSC composite membranes of thickness 1.7 and 1.0 mm. The total electric conductivity for the composite, $\sigma_t = \sigma_i + \sigma_e$, derived from the high-frequency (~10^3 to 10^4 Hz) intercept on the real axis in the impedance diagram, is also presented in Fig. 6. The composite shows a total conductivity of 0.5–1.3 S cm^{-1} at 800–900 °C, which is much larger than the ambipolar conductivity. From combination of σ_t and σ_{amb}, the values for σ_i and σ_e of the composite can be calculated [24]. It is found that σ_e is about two orders of magnitude higher than σ_i, thus $\sigma_i \approx \sigma_{amb}$ and $\sigma_e \approx \sigma_t$. For comparison with the oxygen ionic conductivity of the SDC–LSC composite, the oxygen ionic conductivity of single-phase SDC ceramic determined by impedance spectroscopy in Ref. [25] is also given in Fig. 6. One can see that the former is much smaller than the latter. Even after correction for the volume fraction of the SDC phase in the composite, its oxygen ionic conductivity is still a factor 4–10 smaller than that of single-phase SDC ceramic. This can partly be attributed to the blocking of oxygen ion conducting paths by the LSC phase which is an insulator to oxygen ions [9,10]. It was also found that the transport of oxygen ions in the composite is associated with a larger activation energy as compared with that in the single-phase SDC oxide. The activation energy of σ_i for the composite is calculated to be 154.4 ± 10.4 kJ mol^{-1}, which is about two times larger than that for the single-phase SDC (~82 kJ mol^{-1}) [25]. This may be related to the presence of an ionically resistive layer at the grain boundaries which was likely formed through the diffusion of La and Sr from LSC grain interior to the boundaries between SDC grains [13], and/or from the presence of small amounts of residual $SrCrO_4$ liquid phase formed during sintering [20,26,27].

3.3. Phase composition and microstructure after oxygen permeation measurements

The membranes were examined after oxygen permeation measurements. The examination of XRD patterns taken on both feed and permeate sides of the membrane reveals that SDC and LSC remain as the major phases (Fig. 7). And SEM observation in combination with EDX analysis shows that the microstructure and phase composition of the membrane remain almost unchanged (Fig. 8). These results reveal that no significant reaction occurs between the two constituent oxides during high temperature operation of the membrane. In comparison with the fresh membrane, however, some extra weak peaks are observed in the XRD patterns of the used membrane, and the intensities of these peaks are stronger on its feed side surface than on the permeate side. And a few black grains are found by SEM on the surfaces of the used membrane (Fig. 8a). EDX line-scanning analysis (Fig. 8b–d) reveals that these grains contain mainly Sr and Cr elements as well as minor amounts of La, Ce and Sm. (For simplicity the profiles of Ce and Sm elements are not shown.) The impurity phase observed is not limited to the membrane that underwent high temperature oxygen permeation measurement, which is also found by XRD for the membrane after annealing in air at 1000 °C for 72 h (Fig. 7d). Further analysis reveals that the impurity phase is present only on the surface of the used membrane, but not in the bulk. Probably, the occurrence of the (Sr, Cr)-rich impurity phase is due to the volatilization of the Cr species at high temperatures [27], but not to the reaction between the LSC and SDC oxide in the bulk of the composite membrane.

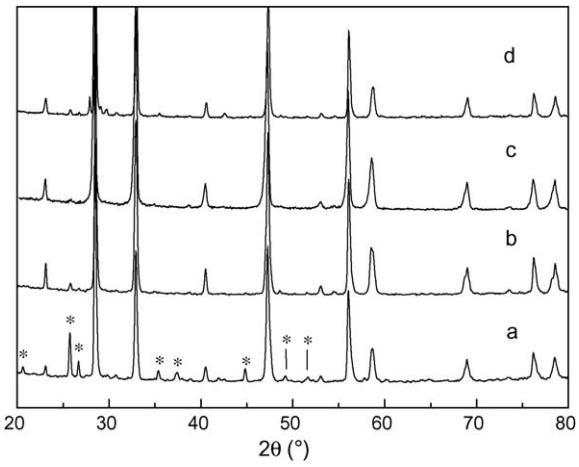

Fig. 7. XRD patterns of composite membranes after oxygen permeation experiments for over 100 h. (a) Feed side; (b) permeate side; (c) polished (bulk); (d) pellet annealed in air at 1000 °C for 72 h. Asterisk (*) represents unknown impurity phase.

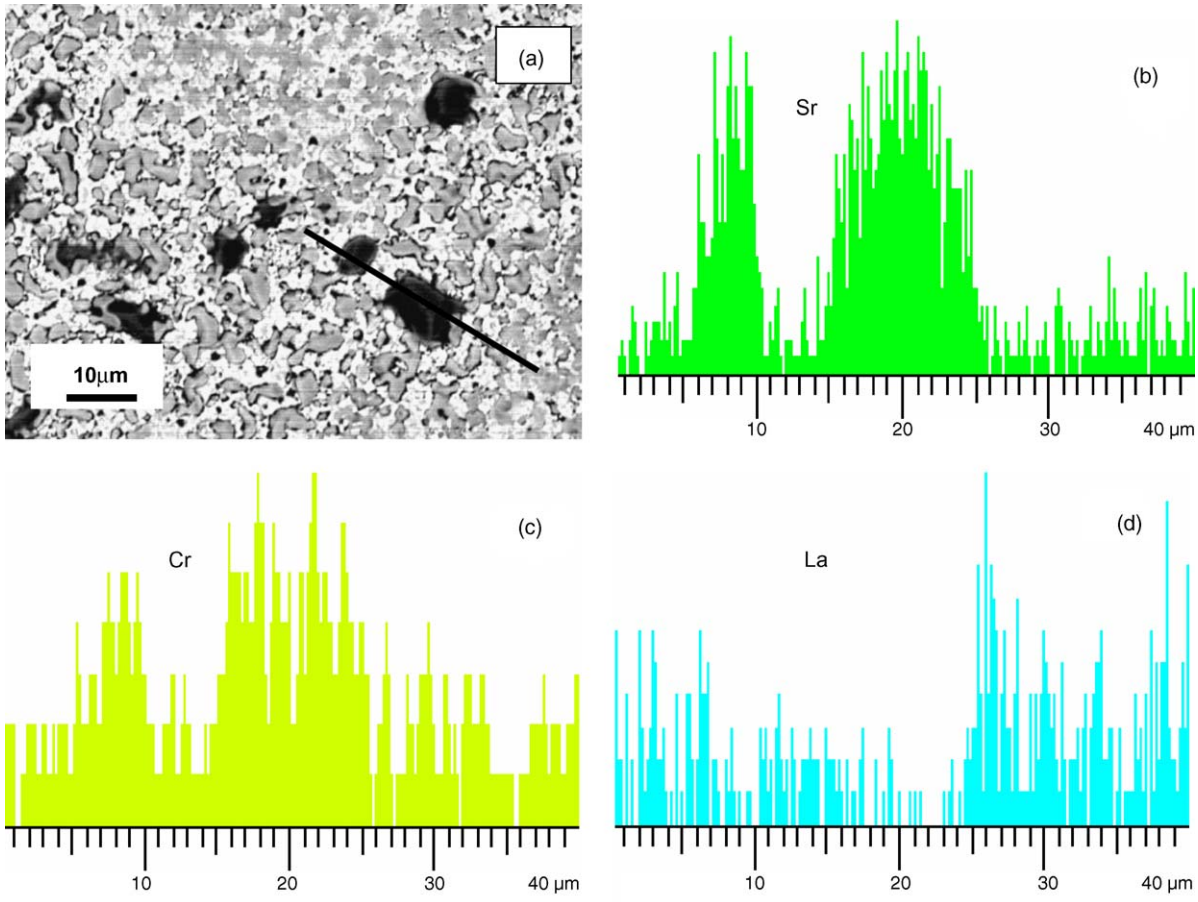

Fig. 8. (a) Backscattered electron image, (b), (c) and (d) EDX line-scanning profile of Sr (La1), Cr (Ka1) and La (La1) for the feed side surface of a membrane after permeation.

4. Discussion

As has been shown above, $Ce_{0.8}Sm_{0.2}O_{2-\delta}$–$La_{0.8}Sr_{0.2}CrO_{3-\delta}$ dual-phase composite possesses substantial and stable oxygen permeability at high temperatures. Moreover, it has also been found recently in the authors' group that this composite exhibits high oxygen fluxes under large oxygen partial pressure gradients and good stability in highly reducing atmospheres. But for practical applications, further improvements are certainly needed including shortening the time for oxygen permeation to reach steady state and increasing the oxygen permeation flux.

The present study shows that the oxygen permeation flux through SDC–LSC increases with time in the initial period and then remains stable. It is suggested that this change in flux does not cause a change in the microstructure of the material, as the process repeats itself after re-equilibrating the system for 85 h (Fig. 3). Both perovskite LSC and fluorite SDC phases are stable under the investigated conditions (Fig. 7), indicating that this "running-in" phenomenon is not a result of any aging (or degradation in oxygen flux) of the material. The constituent oxides $Ce_{0.8}Sm_{0.2}O_{2-\delta}$ and $La_{0.8}Sr_{0.2}CrO_{3-\delta}$ seem to show a better chemical compatibility than $Ce_{0.8}Gd_{0.2}O_{2-\delta}$ and $La_{0.7}Sr_{0.3}MnO_{3-\delta}$. The composite of the latter two oxides was reported to show a decrease in oxygen flux with time (up to 800 h), which was attributed to the reaction between the two oxides [13].

The observation that the "running-in" time required for SDC–LSC dual-phase membrane can be drastically reduced when a porous Pt layer have been applied to both sides of the membrane suggests that this initial process is mainly a surface-controlled one. The porous Pt layer may increase the contact area between the electron-conducting phase LSC and oxygen ion-conducting phase SDC, and thereby shorten the "running-in" time. Possibly, it can also be achieved by reducing the grain size and/or by covering the membrane surface with a porous catalytic layer.

The present study also shows that the overall oxygen permeation process for SDC–LSC composite membrane is mainly controlled by the bulk transport step for membranes with thickness larger than ∼1.0 mm, and at thickness less than ∼0.6 mm the limitation of surface oxygen exchange comes into effect. It is therefore conceivable that further increase in the oxygen flux can be realized through proper design and preparation of the membrane. For example, in the bulk-controlled region, higher oxygen fluxes can be obtained by using thinner membranes and improvement of microstructure. With respect to microstructure, it is known that the presence of dead ends in the oxygen ion conducting phase and large tortuosity of the oxygen ion transport paths, due to the blocking of the electron conducting phase, results in a significant decrease in the ion conductivity of composite membranes [9,10]. Therefore, the ideal way of overcoming this disadvantage is to fabricate a composite in which grains of each phase line up in strings or slabs along the applied oxygen partial pressure gradient. If permeation is controlled by the surface exchange reaction, a higher oxygen flux can also be achieved by means of surface modification as mentioned above.

5. Conclusion

(1) The composite membrane of $Ce_{0.8}Sm_{0.2}O_{2-\delta}$–$La_{0.8}Sr_{0.2}CrO_{3-\delta}$ exhibits considerable oxygen permeability at elevated temperatures. With a 0.3 mm thick membrane, an oxygen permeation flux as large as 1.4×10^{-7} mol cm^{-2} s^{-1} can be obtained upon applying a small oxygen pressure difference at 950 °C. The overall oxygen permeation process is found to be controlled mainly by the bulk transport step for membrane of thickness larger than ∼1.0 mm, and to a large degree by the surface oxygen exchange step at membrane thickness less than ∼0.6 mm.

(2) The oxygen permeation through the membrane is found to increase with time initially, and take a long time to reach a steady state. And applying a porous Pt layer on the membrane surface can shorten the "running-in" period from ∼50 to a few hours, which indicates that the as-observed time-dependent oxygen permeation behavior at the initial stage is due to the activation of surface process and not to the aging of the membrane material.

(3) No observable reaction between two constituent oxides $Ce_{0.8}Sm_{0.2}O_{2-\delta}$ and $La_{0.8}Sr_{0.2}CrO_{3-\delta}$ occurs during the preparation and operation of the membrane at elevated temperatures, making it promising for applications as an oxygen separation membrane.

Acknowledgements

This work was supported by National Natural Science Foundation of China (Grant Nos.: 50332040 and 50225208).

References

[1] P.N. Dyer, R.E. Richards, S.L. Russek, D.M. Taylor, Ion transport membrane technology for oxygen separation and syngas production, Solid State Ionics 134 (2000) 21.
[2] C.S. Chen, S.J. Feng, S. Ran, D.C. Zhu, W. Liu, H.J.M. Bouwmeester, Conversion of methane to syngas by a membrane-based oxidation-reforming process, Angew. Chem. Int. Ed. 42 (2003) 5196.
[3] P.V. Hendriksen, P.H. Larsen, M. Mogensen, F.W. Poulsen, K. Wiik, Prospects and problems of dense oxygen permeable membranes, Catal. Today 56 (2000) 283.
[4] S. Pei, M.S. Kleefisch, T.P. Kobylinski, J. Faber, C.A. Udovich, V. Zhang-McCoy, B. Dabrowski, U. Balachandran, R.L. Mieville, R.B. Poeppel, Failure mechanisms of ceramic membrane reactors in partial oxidation of methane to synthesis gas, Catal. Lett. 30 (1995) 201.
[5] H.H. Wang, Y. Cong, W.S. Yang, Investigation on the partial oxidation of methane to syngas in a tubular $Ba_{0.5}Sr_{0.5}Co_{0.8}Fe_{0.2}O_{3-\delta}$ membrane reactor, Catal. Today 82 (2003) 157.
[6] T. Ishihara, Y. Tsuruta, C.Y. Yu, T. Todaka, H. Nishiguchi, Y. Takita, La(Sr)Ga(Fe)O_3 perovskite oxide as a new mixed ionic–electronic conductor for oxygen permeating membrane, J. Electrochem. Soc. 150 (2003) E17.
[7] Y. Teraoka, H.M. Zhang, S. Furukawa, N. Yamazoe, Oxygen permeation through perovskite-type oxides, Chem. Lett. (1985) 1743.
[8] H. Kruidhof, H.J.M. Bouwmeester, R.H.E. van Doorn, A.J. Burggraaf, Influence of order–disorder transitions on oxygen permeability through selected nonstoichiometric perovskite-type oxides, Solid State Ionics 63–65 (1993) 816.

[9] C.S. Chen, A.J. Burggraaf, Stabilized bismuth oxide–noble metal mixed conducting composites as high temperature oxygen separation membranes, J. Appl. Electrochem. 29 (1999) 355.
[10] K. Wu, S. Xie, G.S. Jiang, W. Liu, C.S. Chen, Oxygen permeation through $(Bi_2O_3)_{0.74}(SrO)_{0.26}$–Ag (40%, v/o) composite, J. Membr. Sci. 188 (2001) 189.
[11] K.Q. Huang, M. Schroeder, J.B. Goodenough, Oxygen permeation through composite oxide-ion and electronic conductors, Electrochem. Solid-State Lett. 2 (1999) 375.
[12] V.V. Kharton, A.V. Kovalevsky, A.P. Viskup, A.L. Shaula, F.M. Figueiredo, E.N. Naumovich, F.M.B. Marques, Oxygen transport in $Ce_{0.8}Gd_{0.2}O_{2-\delta}$-based composite membranes, Solid State Ionics 160 (2003) 247.
[13] V.V. Kharton, A.V. Kovalevsky, A.P. Viskup, F.M. Figueiredo, A.A. Yaremchenko, E.N. Naumovich, F.M.B. Marques, Oxygen permeability of $Ce_{0.8}Gd_{0.2}O_{2-\delta}$–$La_{0.7}Sr_{0.3}MnO_{3-\delta}$ composite membranes, J. Electrochem. Soc. 147 (2000) 2814.
[14] U. Nigge, H.-D. Wiemhöfer, E.W.J. Römer, H.J.M. Bouwmeester, T.R. Schulte, Composites of $Ce_{0.8}Gd_{0.2}O_{1.9}$ and $Gd_{0.7}Ca_{0.3}CoO_{3-\delta}$ as oxygen permeable membranes for exhaust gas sensors, Solid State Ionics 146 (2002) 163.
[15] A.L. Shaula, V.V. Kharton, F.M.B. Marques, Phase interaction and oxygen transport in $La_{0.8}Sr_{0.2}Fe_{0.8}Co_{0.2}O_3$–$(La_{0.9}Sr_{0.1})_{0.98}Ga_{0.8}Mg_{0.2}O_3$ composites, J. Eur. Ceram. Soc. 24 (2004) 2631.
[16] H. Takamura, K. Okumura, Y. Koshino, A. Kamegawa, M. Okada, Oxygen permeation properties of ceria–ferrite-based composites, J. Electroceram. 13 (2004) 613.
[17] H.H. Wang, W.S. Yang, Y. Cong, X.F. Zhu, Y.S. Lin, Structure and oxygen permeability of a dual-phase membrane, J. Membr. Sci. 224 (2003) 107.
[18] M. Mogensen, N.M. Sammes, G.A. Tompsett, Physical, chemical and electrochemical properties of pure and doped ceria, Solid State Ionics 129 (2000) 63.
[19] J.W. Fergus, Lanthanum chromite-based materials for solid oxide fuel cell interconnects, Solid State Ionics 171 (2004) 1.
[20] M. Mori, Y. Hiei, N.M. Sammes, Sintering behavior of Ca- or Sr-doped $LaCrO_3$ perovskites including second phase of $AECrO_4$ (AE = Sr, Ca) in air, Solid State Ionics 135 (2000) 743.
[21] S. Sameshima, T. Ichikawa, M. Kawaminami, Y. Hirata, Thermal and mechanical properties of rare earth-doped ceria ceramics, Mater. Chem. Phys. 61 (1999) 31.
[22] C.E. Hatchwell, N.M. Sammes, G.A. Tompsett, I.W.M. Brown, Chemical compatibility of chromium-based interconnect related materials with doped cerium oxide electrolyte, J. Eur. Ceram. Soc. 19 (1999) 1697.
[23] S. Kim, Y.L. Yang, R. Christoffersen, A.J. Jacobson, Determination of oxygen permeation kinetics in a ceramic membrane based on the composition $SrFeCo_{0.5}O_{3.25-\delta}$, Solid State Ionics 109 (1998) 187.
[24] S. Xie, W. Liu, K. Wu, P.H. Yang, G.Y. Meng, C.S. Chen, Mixed oxygen ionic and electronic conduction in $CaFe_{0.2}Ti_{0.8}O_{3-\delta}$: a combined oxygen permeation and electrical conductivity study, Solid State Ionics 118 (1999) 23.
[25] Z.L. Zhan, T.L. Wen, H.Y. Tu, Z.Y. Lu, AC impedance investigation of samarium-doped ceria, J. Electrochem. Soc. 148 (2001) A427.
[26] J. Sfeir, J. van herle, A.J. McEvoy, Stability of calcium substituted lanthanum chromites used as SOFC anodes for methane oxidation, J. Eur. Ceram. Soc. 19 (1999) 897.
[27] H. Yokokawa, N. Sakai, T. Kawada, M. Dokiya, Chemical thermodynamic considerations in sintering of $LaCrO_3$-based perovskites, J. Electrochem. Soc. 138 (1991) 1018.